

Simple Design Criterion for Residual Energy on Embankment Dam Stepped Spillways

Stefan Felder¹ and Hubert Chanson²

Abstract: The stepped spillway design is associated with significant flow resistance and associated energy dissipation on the steps, yielding smaller, more economical downstream dissipation structures. A number of design guidelines were developed for steep stepped spillways typical of concrete gravity dams. The focus of this study is on embankment stepped spillways. A large set of air-water flow data is compared with reanalyzed data sets to provide a simple unifying design approach for the residual energy at the stepped chute's downstream end and to highlight the uncertainties involved. The results provided some simple design criteria in terms of the dimensionless residual energy of stepped chutes with flat steps. It is believed that a stepped design with a $1V:2.5H$ slope ($\theta = 21.8^\circ$) might be optimum in terms of energy dissipation performances. The Darcy-Weisbach friction factors were close for all stepped data ranging between $0.1 \leq f_e \leq 0.4$. DOI: [10.1061/\(ASCE\)HY.1943-7900.0001107](https://doi.org/10.1061/(ASCE)HY.1943-7900.0001107). © 2015 American Society of Civil Engineers.

Author keyword: Stepped spillways; Embankment dams; Energy dissipation; Residual energy; Flow resistance; Air-water flows; Design method.

Introduction

The stepped chute is a typical spillway design for gravity and embankment dams (Chanson 2001) (Fig. 1). The steps act as rough elements increasing the amount of entrained air and enhancing the rate of energy dissipation along the staircase chute, compared with smooth-invert spillway designs. The strong energy dissipation performances allow a reduction of the downstream stilling structure, reducing construction costs. The flows above stepped spillways are three dimensional. Downstream of the inception point of air-entrainment, the flow appears even more complex with strong air-water flow interactions. Several dissipative processes take place, including cavity recirculations within the step niches driven by momentum transfer from the main stream flow, droplet ejections above the air-water flows, and strong turbulent energetic processes within the bulk of the two-phase flow (Matos 2001; Chanson et al. 2002; Ohtsu et al. 2004). The investigation of the energetic processes is closely linked with the air-water flows, and the energy dissipation rate should be measured directly in the two-phase flow section at the downstream end of the stepped chute.

Although the energy dissipation processes on steeply sloped stepped spillways have been studied in great details, the focus shifted during the last decade to the study of spillways with typical embankment dam slopes $\theta \leq 30^\circ$. Some studies provided important information about the flow patterns and monophasic flow processes (Amador et al. 2006; Meireles and Matos 2009; Hunt and Kadavy 2010; Frizell et al. 2013). Further studies focused on the air-water flow parameters providing details about the air-water flow processes on the basis of measurements with phase-detection intrusive

probes (e.g., Chanson and Toombes 2002a, b; Ohtsu et al. 2004; Gonzalez and Chanson 2008; Carosi and Chanson 2008; Thorwarth 2008; Felder and Chanson 2009; Bung 2009; Takahashi and Ohtsu 2012; Felder 2013; Guenther et al. 2013).

A number of design guidelines for embankment chute were developed on the basis of air-water flow experiments, including Ohtsu et al. (2004) for $5.7^\circ < \theta < 19^\circ$, Gonzalez and Chanson (2007) for $\theta = 15.9^\circ$ and 21.8° , and Bung (2011) on stepped chutes with $\theta = 18.4^\circ$ and 26.6° . Recently, Hunt et al. (2014) provided guidelines for stepped chutes with slopes of $14^\circ \leq \theta \leq 26.6^\circ$ on the basis of experiments with monophasic flow and air-water flow devices. Each set of design guidelines is based on the respective experimental data collected in stepped chutes with various slopes, channel geometries, inflow conditions, flow rates, and instrumentation. Interestingly, the resulting guidelines are fairly similar, often with slight differences in empirical factors in same or similar equation format. These differences are the consequence of different experimental results sometimes even for the same channel slope. There is a need to provide clarity on the uncertainty of the design guidelines.

The present work is an approach to use the available air-water flow data to provide a simple unifying design approach for the residual energy at the chute's downstream end and to highlight the uncertainties involved. The basis of the present paper are extensive measurements by Felder (2013) of the air-water flow properties on several stepped configurations with typical embankment dam slopes of $\theta = 26.6^\circ$ and $\theta = 8.9^\circ$ (Fig. 2). These results are complemented with the reanalyses of a number of detailed air-water stepped spillway data on flat slopes of $3.4^\circ \leq \theta \leq 26.6^\circ$, providing a new design criterion for the residual energy at the downstream end of the stepped section.

Experimental Data Set and Configurations

Physical experiments were conducted in three large stepped spillway models encompassing a range of stepped geometries, i.e., flat uniform steps, flat nonuniform steps, pooled steps, porous pooled steps, and combination of flat and pooled steps (Table 1). Fig. 2 illustrates the investigated configurations with vertical step heights,

¹Lecturer, Water Research Laboratory, School of Civil and Environmental Engineering, UNSW Australia, 110 King St., Manly Vale, NSW 2093, Australia (corresponding author). E-mail: felder@unsw.edu.au

²Professor, School of Civil Engineering, Univ. of Queensland, Brisbane QLD 4072, Australia. E-mail: h.chanson@uq.edu.au

Note. This manuscript was submitted on November 25, 2014; approved on September 15, 2015; published online on November 19, 2015. Discussion period open until April 19, 2016; separate discussions must be submitted for individual papers. This paper is part of the *Journal of Hydraulic Engineering*, © ASCE, ISSN 0733-9429.



(a)



(b)

Fig. 1. Prototype stepped spillways (images by Hubert Chanson): (a) Hinze dam stepped spillway and stilling basin, Gold Coast, Australia, on October 24, 2014; (b) stepped spillway of Gold Creek embankment dam, Brisbane, Australia, on December 27, 2010

$h = 0.05$ and 0.10 m, and vertical drop in elevation between upstream broad-crested weir and last step edge, $\Delta z_o = 0.9$ and 1 m. For all stepped configurations, the uncontrolled broad-crested weir provided a smooth inflow into the stepped test section with widths of $W = 0.5, 0.52,$ and 1.0 m, respectively. On the spillway with $\theta = 8.9^\circ$, the pooled stepped configurations consisted of weirs at the step edge of height $w = 5$ cm. On the steeper sloped spillway with $\theta = 26.6^\circ$, the pooled weirs had $w = 3.1$ cm to satisfy the same $w:l$ ratio of pool weir height to step length between the pooled configurations. For two pooled designs, a pool weir porosity was added ($P_o = 5$ and 31%) to simulate pooled designs with low-flow drainage and gabion permeability, respectively (Fig. 2). Details about the configuration with step pool porosity can be found in Felder and Chanson (2014b). The experimental flow conditions are summarized in Table 1 including the discharge per unit width between $0.003 \leq q_w \leq 0.267$ m²/s and the dimensionless discharge d_c/h , where d_c is the critical flow depth. The discharges corresponded to Reynolds numbers within two orders of magnitude: $1.5 \times 10^4 \leq R \leq 1.1 \times 10^6$. The Reynolds number was defined in terms of the hydraulic diameter. The flow patterns of all stepped chutes were investigated, including the inception point of free-surface aeration and the air-water flow characteristics (Felder 2013).

A key characteristic of stepped spillways is the large rate of energy dissipation along the stepped chute associated with a strong air entrainment downstream of the inception point of free-surface aeration. Hence, experiments on stepped spillways must describe the air-water flow properties and the energy dissipation characteristics in the two-phase flow region. In the present study, detailed air-water flow measurements were performed with dual-tip phase-detection probes with probe sensor sizes $\varnothing = 0.13$ and 0.25 mm for a range of discharges corresponding to the transition and skimming flow regimes ($0.69 \leq d_c/h \leq 3.55$). The conductivity probes were sampled at 20 kHz per sensor for 45 s at all step edges downstream of the inception point of free-surface aeration. The air-water data processing followed the method of Chanson (2002) and Felder (2013).

The present data used for the design criterion comprised a range of flow rates of $0.035 \leq q_w \leq 0.234$ m²/s for flat uniform steps on the stepped spillway with $\theta = 8.9^\circ$ and for $0.02 \leq q_w \leq 0.186$ m²/s for flat steps with $\theta = 26.6^\circ$ because the last step edge had to be at least three step edges downstream of the inception point

of air entrainment. The present data were compared with several stepped spillway data sets with slopes between $3.4^\circ \leq \theta \leq 26.6^\circ$ (Table 2). These studies were also conducted with phase-detection probes to document the air-water flow properties and the energy dissipation performances. Table 2 lists the relevant studies including the channel slope, stepped configuration, step heights, height between upstream end and last step edge, and probe sensor size. The comparative analyses provided a comprehensive experimental data set to assess the energy dissipation performances for embankment stepped spillways, leading to a simple design criterion for the residual energy at the spillway toe. At the downstream end of the spillways the air-water flows were fully developed, but no uniform equilibrium flow conditions were observed. The data of Hunt et al. (2014) are not included because it was not possible to differentiate between air-water flow data and monophasic flow data, and the data corresponding to the spillway toe.

Air-Water Flow Patterns

For all present stepped configurations, the flow patterns were observed for a range of discharges comprising nappe (NA), transition (TRA), and skimming flow (SK) regimes (Table 1). In the nappe flow regime for small discharges, the water discharged from one step to the next in a series of free-falling nappes. For intermediate flow rates, a transition flow regime existed, which consisted of slight instabilities visible in strong droplet splashing and irregular cavity recirculation for the flat stepped spillways. For the pooled stepped design, stronger instabilities were observed within the transition flows consisting of jump waves and flow instabilities (Felder and Chanson 2013). In particular for the pooled stepped design with $\theta = 8.9^\circ$, a safe operation of the spillway might not be possible because of strong instationary flow patterns including jump waves propagating downstream [Fig. 3(a)]. For the largest flow rates, typically the design discharge, a skimming flow regime was observed [Figs. 3(b and c)]. At the upstream end, a clear water region existed, and when the turbulence fluctuations within the flow were large enough to overcome the surface tension and buoyancy forces, the air entrainment process started. A highly-complex three-dimensional air-water flow mixture was observed downstream [Figs. 3(b and c)].

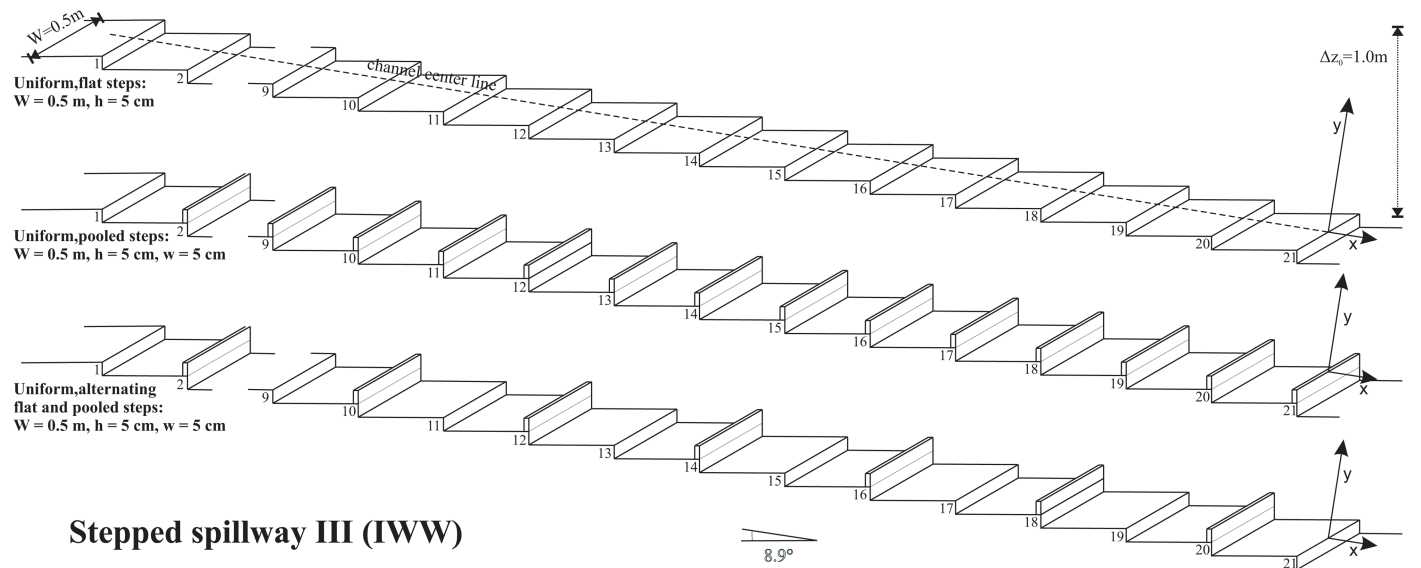
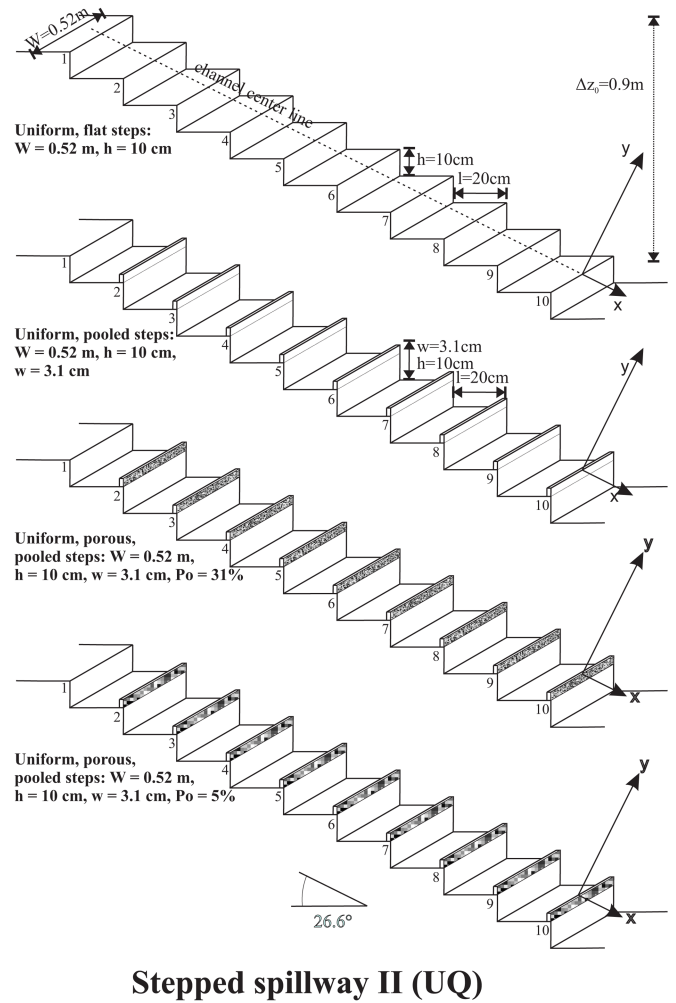
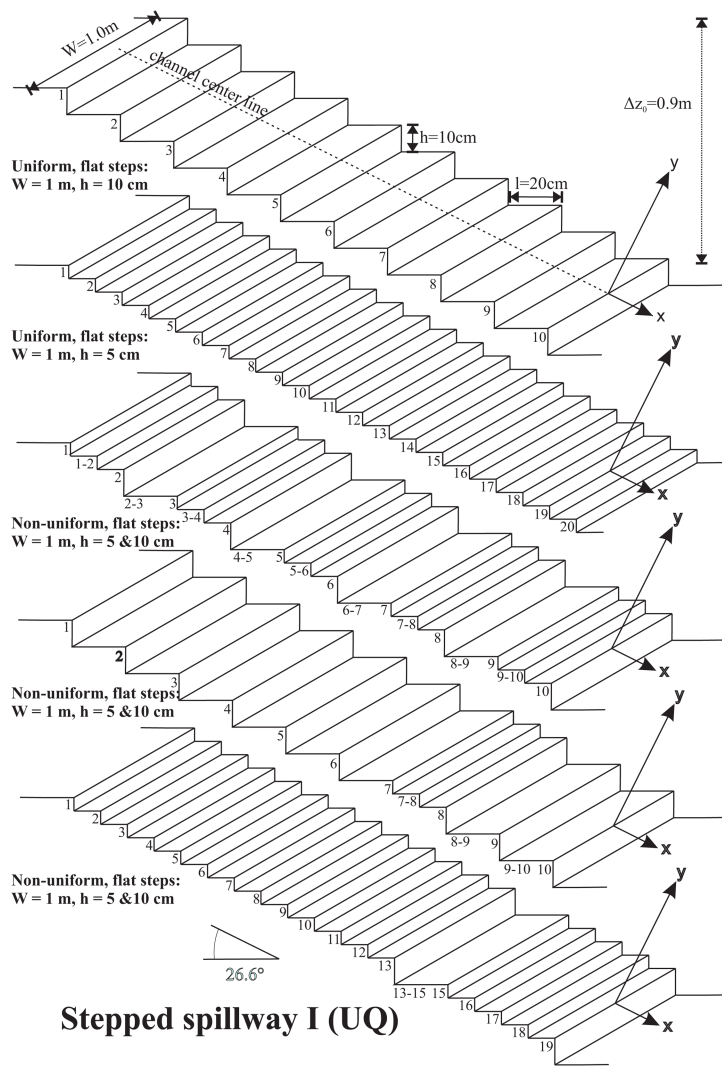


Fig. 2. Dimensioned sketches of stepped configurations (present study): measurements with double-tip conductivity probes

The positions of the inception point of free-surface aeration were observed for all flow conditions and stepped configurations. The smooth stepped chute data were in close agreement and well fitted by existing correlation functions from the literature

(Felder and Chanson 2013) such as the simple correlation by Chanson (1994, 2001)

$$\frac{L_I}{h \times \cos \theta} = 9.719 \times (\sin \theta)^{0.0796} \times F^{0.713} \quad (1)$$

Table 1. Summary of Experimental Flow Conditions of Stepped Spillway Configurations in Present Study (Fig. 2)

Slope	Stepped configuration (h and w in cm)	Δz_o (m)	Conductivity probe	q_w (m ² /s)	d_c/h [-]	d_c/h [-]	d_c/h [-]
						NA—TRA	TRA—SK
8.9°	$h = 5$ (flat)	1.0	Double-tip ($\varnothing = 0.13$ mm)	0.004–0.234	0.24–3.54	0.95	1.69
	$h = w = 5$ (pooled)			0.009–0.233	0.39–3.54	1.08	1.76
	$h = w = 5$ (flat/pooled)			0.007–0.233	0.52–3.54	1.0	N/A
26.6°	$h = 10$ (flat)	0.9	Double-tip ($\varnothing = 0.25$ mm)	0.008–0.262	0.18–1.91	0.58	0.9
	$h = 5$ (flat)			0.005–0.230	0.27–3.51	0.53	1.06
	$h = 5$ and 10 (nonuniform)	0.9		0.005–0.241	0.13–1.81	0.53	0.97 (1.7 for 5 cm dominating)
	$h = 10, w = 3.1$ (pooled)	0.87		0.004–0.267	0.11–1.94	0.45	0.97
	$h = 10, w = 3.1, P_o = 31\%$ (porous pooled)	0.87		0.003–0.282	0.10–2.01	0.43	0.75
	$h = 10, w = 3.1, P_o = 5\%$ (porous pooled)	0.87		0.003–0.282	0.10–2.01	0.46	0.91

Table 2. Summary of Previous Air-Water Flow Studies on Stepped Spillways with Embankment Dam Slopes

Slope	Stepped configuration (h and w in cm)	Spillway height, Δz_o (m)	Conductivity probe, (\varnothing in mm)	Reference
3.4°	$h = 7.15$ (flat)	1.14	Single-tip ($\varnothing = 0.35$)	Chanson and Toombes (2002b)
	$h = 14.3$ (flat)			
5.7°	$h = 0.63$ –5 (flat)	0.3–0.7	Single-tip ($\varnothing = 0.1$)	Ohtsu et al. (2004)
8.9°	$h = 5$ (flat)	1	Double-tip ($\varnothing = 0.13$)	Thorwarth (2008)
	$h = w = 5$ (pooled)	0.95		
11.3°	$h = 0.63$ –5 (flat)	0.3–0.7	Single-tip ($\varnothing = 0.1$)	Ohtsu et al. (2004)
14.6°	$h = 5$ (flat)	1	Double-tip ($\varnothing = 0.13$)	Thorwarth (2008)
	$h = 10$ (flat)			
15.9°	$h = w = 5$ (pooled)	0.95		
15.9°	$h = 5$ (flat)	0.8	Double-tip ($\varnothing = 0.025$)	Gonzalez (2005)
	$h = 10$ (flat)			Chanson and Toombes (2002a)
18.4°	$h = 3$ (flat)	2.34	Double-tip ($\varnothing = 0.13$)	Bung (2009)
	$h = 6$ (flat)			
19°	$h = 0.63$ –5 (flat)	0.85–2.4	Single-tip ($\varnothing = 0.1$)	Ohtsu et al. (2004)
21.8°	$h = 5$ (flat)	0.95	Double-tip ($\varnothing = 0.25$)	Felder and Chanson (2009)
	$h = 10$ (flat)	0.9	Double-tip ($\varnothing = 0.25$)	Carosi and Chanson (2008)
26.6°		0.8	Single-tip ($\varnothing = 0.35$)	
		0.7	Double-tip ($\varnothing = 0.025$)	Gonzalez (2005)
	$h = 3$ (flat)	2.34	Double-tip ($\varnothing = 0.13$)	Chanson and Toombes (2002a)
	$h = 6$ (flat)		Double-tip ($\varnothing = 0.13$)	Bung (2009)
	$h = 10, w = 3.1$ (in-line flat/pooled steps)	0.9	Double-tip ($\varnothing = 0.25$)	Guenther et al. (2013)
	$h = 10, w = 3.1$ (staggered flat/pooled steps)			

where L_I = distance from the first step edge to the inception point of free-surface aeration; and F^* = Froude number expressed in terms of the step roughness

$$F^* = \frac{q_w}{\sqrt{g \times \sin \theta \times k_s^3}} \quad (2)$$

where g = gravity acceleration; and k_s = step cavity height normal to the mainstream flow: $k_s = h \times \cos \theta$ for flat stepped spillways and $k_s = (h + w) \times \cos \theta$ for pooled stepped spillways. For the pooled stepped data, a slightly different correlation proposed by Thorwarth (2008) matched the pooled data well. The agreement between equations and experimental data is not shown because it has been presented previously (Felder and Chanson 2013). Felder and Chanson (2013) compared their correlation and data set [Eq. (1)] with several other formulas including Meireles and Matos (2009) and Hunt et al. (2014). There is close agreement between the formulas and experimental data available.

Similarly, several empirical formulas describe the flow depth in the clear-water flow region d_w above the inception point

(e.g., Meireles and Matos 2009; Hunt et al. 2014). Chanson (2001) developed a semiempirical equation for the flow depth on the basis of boundary layer development thickness δ_{BL}

$$d_w = \frac{q_w}{\sqrt{2 \times g \times (H_{\max} - d_w \times \cos \theta)}} + \frac{\delta_{BL}}{N} \quad (3)$$

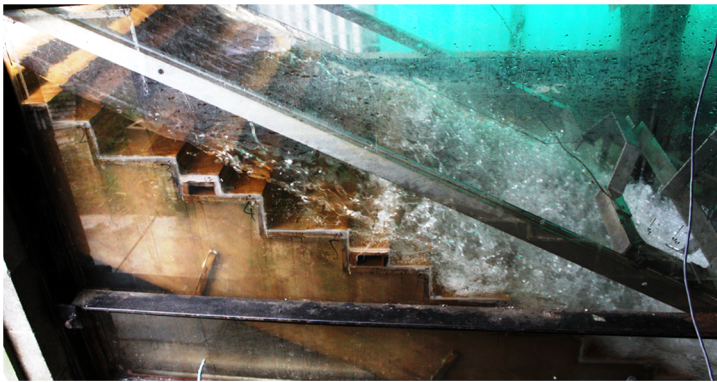
Eq. (3) was successfully tested by Chanson (2001) and Felder and Chanson (2014a). Because of its semiempirical nature, Eq. (3) should receive preference above solely empirical equations.

Air-Water Flow Properties

The air-water flow properties were measured for all stepped configurations at all step edges downstream of the inception point. Characteristic results of several air-water flow properties are presented in this section comprising the vertical distributions of void fraction C and interfacial velocity V (Fig. 4) and the longitudinal development of characteristic air-water flow parameters (Fig. 5).



(a)

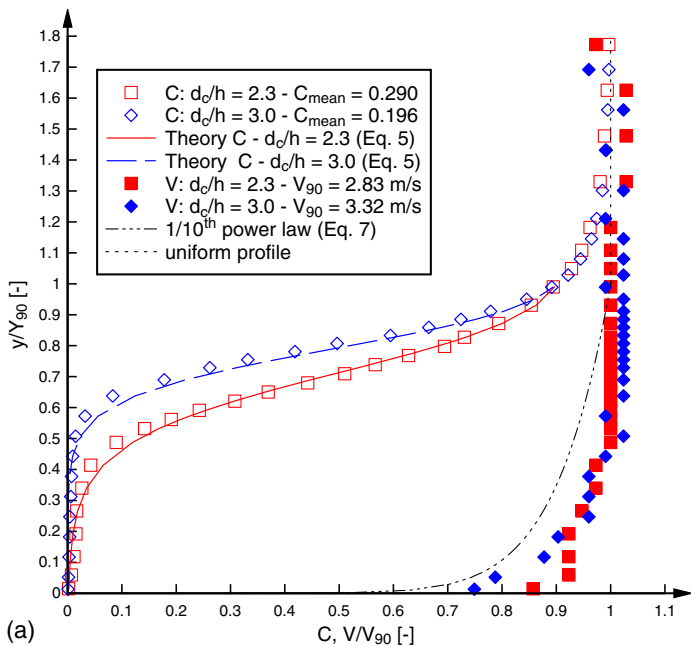


(b)

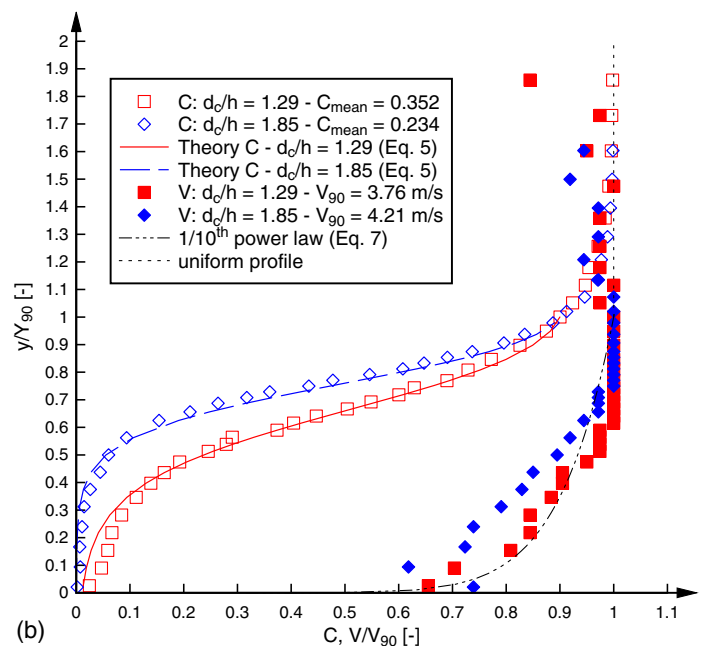


(c)

Fig. 3. Air-water flow patterns on stepped spillways with embankment dam slopes: (a) transition flows on nonuniform pooled stepped spillway $\theta = 8.9^\circ$: $d_c/h = 3.34$, $q_w = 0.214 \text{ m}^3/\text{s}$, $R = 8.49 \times 10^5$; (b) skimming flows on nonuniform flat stepped spillway $\theta = 26.6^\circ$: $d_c/h = 1.22$, $q_w = 0.133 \text{ m}^2/\text{s}$, $R = 5.3 \times 10^5$; (c) skimming flows on pooled stepped spillway $\theta = 26.6^\circ$: $d_c/h = 1.27$, $q_w = 0.142 \text{ m}^2/\text{s}$, $R = 5.6 \times 10^5$



(a)



(b)

Fig. 4. Dimensionless distributions of air-water flow properties at the downstream end of stepped spillways with flat and pooled uniform steps—comparison with advective diffusion equation [Eq. (5)] and power law [Eq. (7)]: (a) flat uniform steps $h = 5 \text{ cm}$, $\theta = 8.9^\circ$: void fraction and interfacial velocity; (b) pooled uniform steps $h = 10 \text{ cm}$, $w = 3.1 \text{ cm}$, $\theta = 26.6^\circ$: void fraction and interfacial velocity

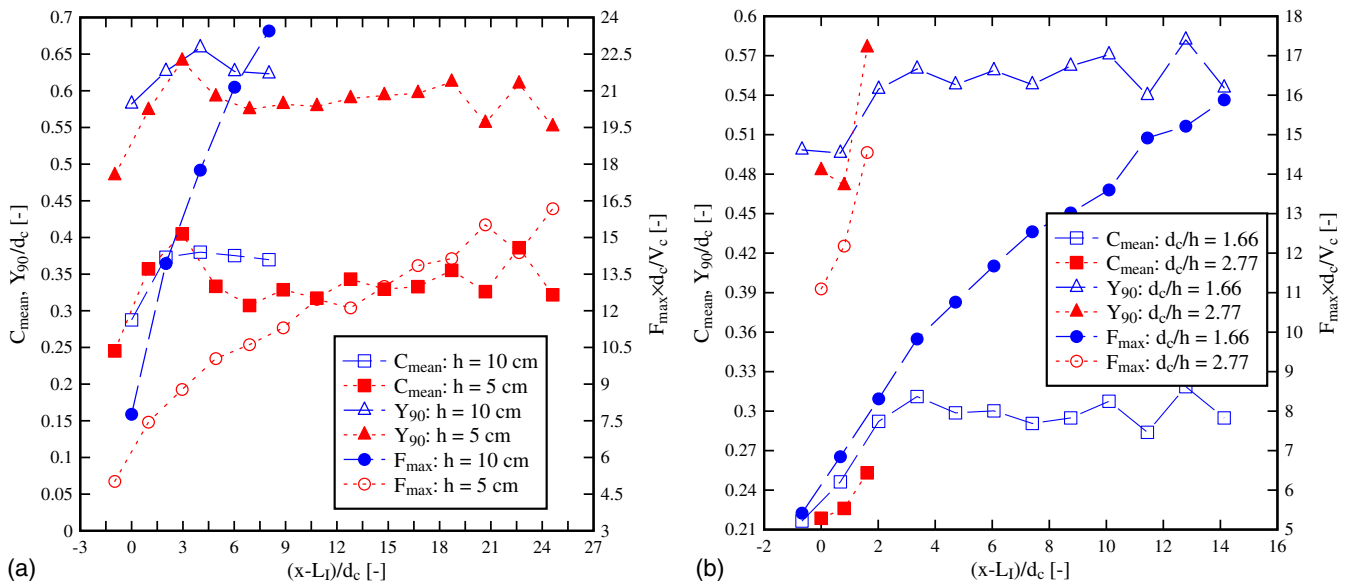


Fig. 5. Longitudinal dimensionless distributions of characteristic air-water depth Y_{90}/d_c , velocity V_{90}/V_c , and maximum bubble count rate $F_{\max}d_c/V_c$: (a) flat uniform steps $h = 5$ and 10 cm, $\theta = 26.6^\circ$: $d_c/h = 1.11$, $q_w = 0.116$ m²/s, $R = 4.6 \times 10^5$; (b) flat uniform steps $h = 5$ cm, $\theta = 26.6^\circ$: $d_c/h = 1.66$, $q_w = 0.075$ m²/s, $R = 3.0 \times 10^5$ and $d_c/h = 2.77$, $q_w = 0.161$ m²/s, $R = 6.4 \times 10^5$

Typical skimming flow distributions of local time-averaged void fraction C above the stepped chute are illustrated in Fig. 4 for two-channel slopes and different discharges. In the figure legend, the depth-average air concentration C_{mean} is added

$$C_{\text{mean}} = \frac{1}{Y_{90}} \int_{y=0}^{y=Y_{90}} C \times dy \quad (4)$$

where y = distance perpendicular to the mainstream flow direction; Y_{90} = characteristic distance, where $C = 0.9$; and C_{mean} = key parameter for the theoretical solution of the void fraction distributions, i.e., the advective diffusion equation for air bubbles in air-water skimming flows

$$C = 1 - \tanh^2 \left[K' - \frac{y/Y_{90}}{2 \times D_o} + \frac{(y/Y_{90} - 1/3)^3}{3 \times D_o} \right] \quad (5)$$

where K' and D_o = dimensionless functions of C_{mean} only (Chanson and Toombes 2002a). In Fig. 4, Eq. (5) compares favorably with the experimental void fraction data. Close agreement between the advective diffusion equation [Eq. (5)] and experimental data has been also confirmed in many other air-water flow studies of embankment dam sloped stepped spillways whereas void fraction profiles in less stable transition flows are well correlated by a different solution of the same advective diffusion equation (Chanson and Toombes 2004). In the uniform equilibrium flow region, the mean air concentration C_{mean} can be estimated with an empirical equation by Ohtsu et al. (2004)

$$C_{\text{mean}} = D - 0.3 \exp \left[-5 \left(\frac{h}{d_c} \right)^2 - 4 \frac{h}{d_c} \right] \quad (6)$$

where $D = 0.3$ for $5.7^\circ \leq \theta \leq 19^\circ$; and $D = -0.00024\theta^2 + 0.0214\theta - 0.0357$ for $\theta \geq 19^\circ$. Again various other empirical formulas exist.

Typical time-averaged interfacial velocity distributions are also illustrated in Fig. 4 for the same flow conditions. The dimensionless interfacial velocity distributions V/V_{90} compared well with a power law

$$\frac{V}{V_{90}} = \left(\frac{y}{Y_{90}} \right)^{1/N} \quad y/Y_{90} \leq 1 \quad (7)$$

where V_{90} = velocity with $C = 0.90$; and N = power law coefficient, typically $N = 10$ for stepped chutes. Variations in parameters of N have been observed by several researchers (e.g., Bung 2011; Takahashi and Ohtsu 2012; Hunt et al. 2014). As seen in Fig. 4, there are small deviations from the 1/10th power law linked to variations between adjacent step edges, with distance downstream of the inception point, with variation in step configuration and discharges. The factor $N = 10$ reflected an average power law coefficient for the observations by Felder (2013) for the full range of stepped configurations and discharges for the present data sets (Fig. 2). Differences in factor N might be also explained with different experimental facilities, measurement devices, and sampling parameters, but reflect most importantly the complexity and fluctuations of the three-dimensional flow. For $y/Y_{90} > 1$, the interfacial velocities followed a quasi-uniform profile for all flow conditions, but for some flow rates, uniform velocities were seen for $y/Y_{90} > 0.7$ (Fig. 4). In the legend of Fig. 4, the values of V_{90} are also presented for completeness. Similar distributions of void fractions and interfacial velocities were recorded for all stepped configurations, confirming such features as characteristic for air-water skimming flows independently of step height, embankment dam slope, and downstream distance from the inception point of air entrainment.

Characteristic air-water flow parameters were also estimated for all step edges downstream of the inception point of free-surface aeration. These parameters comprised the maximum bubble count rate F_{\max} , i.e., the maximum number of air bubbles in a cross section, the mean void fraction in a cross section C_{mean} , and the characteristic flow depth Y_{90} . The flow parameters are illustrated in dimensionless terms in Fig. 5 as a function of the dimensionless distance from the inception point $(x - L_I)/d_c$, where x is the distance along the spillway. The longitudinal distributions of the air-water flow properties highlighted the rapidly varying flow region immediately downstream of the inception point of air entrainment. Further downstream, the flow parameters vary gradually and no uniform flow conditions were observed on the present spillway

facilities. In particular the dimensionless maximum bubble count rate $F_{\max} V_c / d_c$ did increase gradually along the spillway (Fig. 5), where V_c is the critical flow velocity. Furthermore, all air-water flow parameters showed a seesaw patterns, which may be typical for stepped spillway flows as shown by Felder and Chanson (2009). Fig. 5 confirms that no uniform equilibrium conditions were achieved at the downstream end of the stepped chute and that the flow was fully developed air-water flows, which varied gradually for all configurations. Because of the rapidly varied flow in the region just downstream of the inception point, the design criterion of the present study is only valid for positions at least three step edges downstream of the inception point of air entrainment. Data that did not fulfill this three step rule were not considered for the calculation of the median dimensional residual energy. For several flow conditions, residual energies were observed for consecutive step edges, showing very similar residual energy levels independent of the height of the step edge to the weir crest. Although the residual energy at consecutive steps would have provided additional experimental data, only the residual energy at the downstream end of the chutes were considered for the design criterion. This was done for consistency with flow configurations in which only the residual energy at the downstream end was available.

Energy Dissipation and Flow Resistance

Residual Energy for Flat Sloped Stepped Spillways

The present air-water flow data were used to calculate some key design parameters, namely, the residual energy at the last step edge at the chute's downstream end and the average friction factor in the fully developed air-water flow region. The residual energy at the chute's downstream end is an important design parameter for the downstream energy dissipator, typically a stilling basin. The size of this stilling basin must be designed to allow the dissipation of the remaining energy to avoid damage and erosion of the river further downstream. The present data were compared with the reanalysis of existing air-water flow data for embankment dam slopes to provide guidance for a large range of channel slopes and configurations and to combine data from different facilities (Table 2). The residual head at the downstream end is calculated on the basis of air-water flow data as

$$H_{\text{res}} = d \times \cos \theta + \frac{U_w^2}{2 \times g} + w = \int_0^{y_{90}} (1 - C) \times \cos \theta \times dy + \frac{q_w^2}{2 \times g \times [\int_0^{y_{90}} (1 - C) \times dy]^2} + w \quad (8)$$

where d = equivalent clear water flow depth; U_w = depth average velocity; g = gravity acceleration; and w = pool weir height (for pooled and porous pooled stepped spillways only). For the staggered and in-line configurations of flat and pooled stepped spillways, a cross-sectional averaging was used following Guenther et al. (2013). Fig. 6 presents the dimensionless residual energy H_{res}/d_c data as functions of the dimensionless discharge d_c/h . The present data are highlighted with filled symbols, and the reanalyzed data are shown as hollow symbols. The data are presented in four graphs, regrouping stepped spillway data with similar channel slopes (Fig. 6). The comparative analysis identified four stepped spillway slopes exhibiting similar dimensionless residual energy results: $3.4^\circ \leq \theta \leq 11.3^\circ$; $14.6^\circ \leq \theta \leq 19^\circ$; $\theta = 21.8^\circ$; and $\theta = 26.6^\circ$. For each group, the median values and the standard deviation

of data are included with solid and dashed lines, respectively (Fig. 6).

Fig. 6(a) shows the residual energy for flat and pooled stepped spillways with $3.4^\circ \leq \theta \leq 11.3^\circ$, the median values for the flat stepped data ($H_{\text{res}}/d_c = 3.31$) for all channel slopes, and the median values for the pooled stepped spillway data with $\theta = 8.9^\circ$ ($H_{\text{res}}/d_c = 2.28$). Although the pooled design might be better in terms of energy dissipation performances, its safe operation is not advised because of instationary free-surface jump waves (Takahashi et al. 2008; Felder and Chanson 2013). Fig. 6(b) illustrates the residual energy for $14.6^\circ \leq \theta \leq 19^\circ$, the median dimensionless residual energy $H_{\text{res}}/d_c = 3.96$, and the standard deviation of the data. In Fig. 6(c), the residual head data for flat steps with 21.8° are shown together with the median residual energy $H_{\text{res}}/d_c = 3.37$. The data showed some scatter, most notably for the data with $h = 0.10$ m, and the large standard deviation reflect the scatter. The data set comprised experimental results from three different studies (Table 2) conducted with different probe sensor sizes and variations in sampling parameters. It is conceivable that the smallest sensors yielded larger residual energy values. A more detailed study could provide insights on any effect of sensor sizes on air-water flow properties and energy dissipation rates. The largest values of residual energy were observed for transition flow discharges, i.e., discharges below the design skimming flow discharge, which are characterized by instabilities. The fourth group of data ($\theta = 26.6^\circ$) is shown in Fig. 6(d) comprising data for flat uniform, flat nonuniform, pooled steps, and porous pooled steps, and configurations of in-line and staggered configurations of flat and pooled steps. The median residual energy and the standard deviation are also shown for the flat stepped data (both uniform and nonuniform configurations) ($H_{\text{res}}/d_c = 3.94$). The pooled and porous pooled stepped spillway configurations showed the largest residual energy levels, and the design might not be beneficial in terms of energy dissipation performances because the rate of energy dissipation is closely linked with the residual energy at the downstream end. Again, the largest residual energies were observed for instable transition flows.

Fig. 7 summarizes the median residual energy values as functions of the spillway slope for all data presented in Fig. 6. The standard deviation of experimental data is added to the figure with error bars. The results demonstrate a similar order of magnitude in terms of median residual energies for all four stepped spillway groups. Furthermore, they indicated a slight increase of residual energy with increasing channel slope, but the data for $\theta = 21.8^\circ$ indicated a drop in residual energy for that particular slope. Such a stepped spillway slope might be best in terms of energy dissipation performances for embankment stepped chute slopes within the range of $14.6^\circ \leq \theta \leq 26.6^\circ$ (Fig. 7). This finding was close to the results of Ohtsu et al. (2004) and Gonzalez and Chanson (2006). Very flat slopes might yield smaller residual energy levels at the chute toe, but the design would yield long and uneconomical designs.

A relatively close agreement was obtained between all experimental data, with a majority within the range of $2 \leq H_{\text{res}}/d_c \leq 5$. The median residual energies for four groups with similar slopes were calculated, highlighting typical residual energies usable as simple design criterion. Table 3 summarizes the design criteria for embankment stepped spillways with slopes within $3.4^\circ \leq \theta \leq 26.6^\circ$ incorporating the present data (Table 1) and previous air-water flow studies on stepped spillways (Table 2). The guidelines are valid for uniform flat steps within a range of step heights and discharges in both transition and skimming flow regimes. No uniform equilibrium conditions were observed at the downstream end, and the design guidelines are valid for fully developed air-water

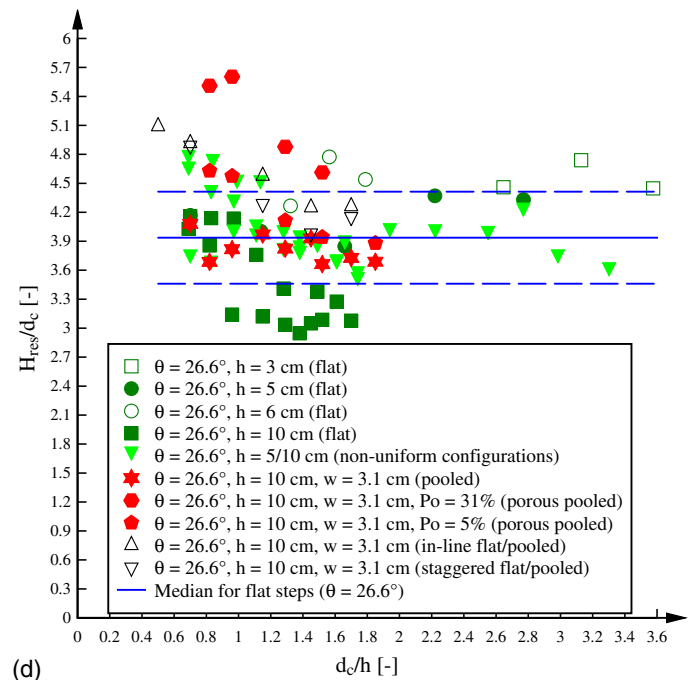
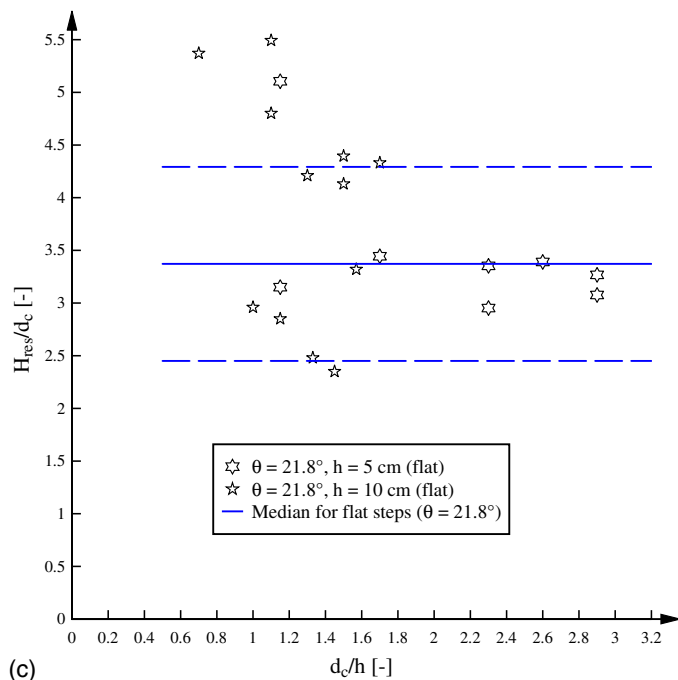
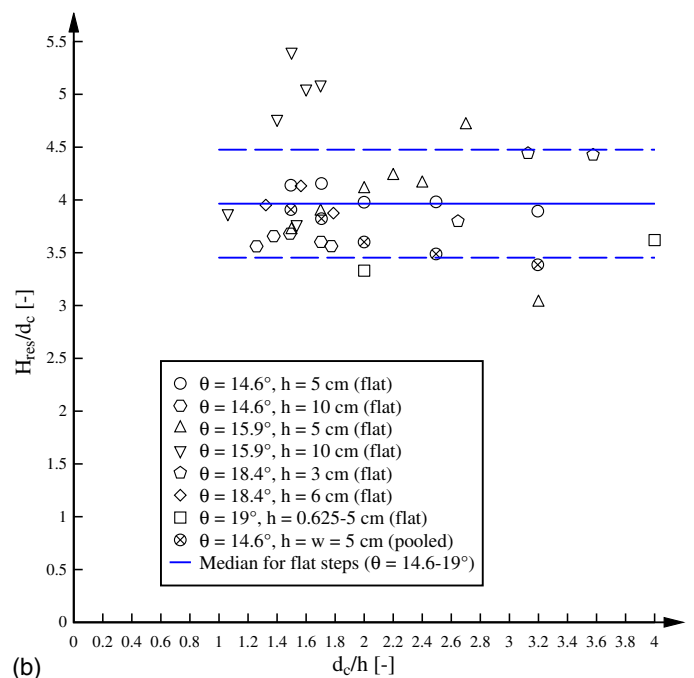
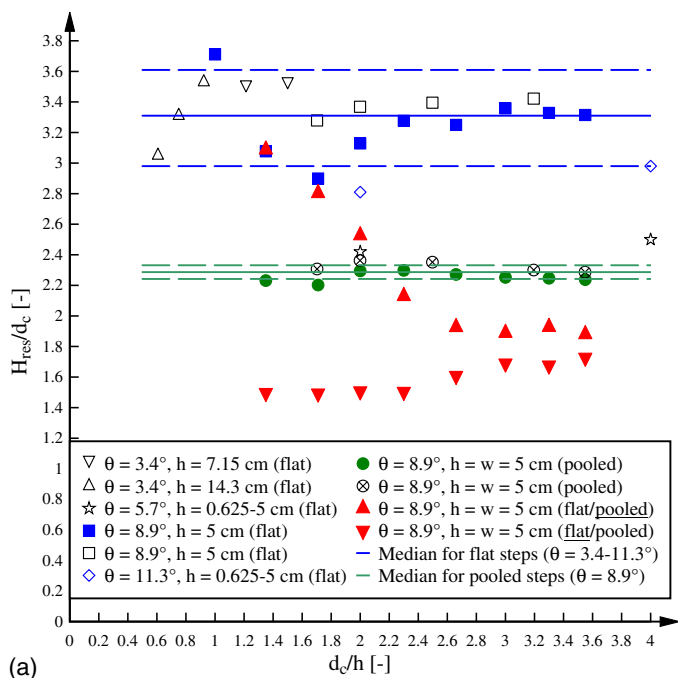


Fig. 6. Dimensionless residual energy at the downstream end of stepped spillways with embankment dam slopes; filled symbols = present data, Table 1; hollow symbols = Table 2; solid line = median values for design guidelines; dashed lines = standard deviation of data: (a) residual energy and median values for flat and pooled steps with $3.4^\circ \leq \theta \leq 11.3^\circ$; (b) residual energy and median values for flat and pooled steps with $14.6^\circ \leq \theta \leq 19^\circ$; (c) residual energy and median values for flat and pooled steps with $\theta = 21.8^\circ$; (d) residual energy and median values for flat and pooled steps with $\theta = 26.6^\circ$

flows with nonuniform flow conditions. A benefit of such design guidelines is the simplicity for application to the full range of flat sloped spillways.

Discussion

Although the design criterion for embankment sloped stepped spillways is straightforward, the presented data highlight also a

weakness of today's research in air-water stepped spillway flows. A large scatter of experimentally observed data was shown in Figs. 6 and 7, which results in large uncertainties of the actual residual energy at the downstream end. In the present paper, the effort was to include as many air-water flow data as possible for the analyses to find a design criterion that is valid independently of the experimental facility and the instrumentation used for data collection. Using a median value as the representative residual head at the downstream end represents a typical value for the available

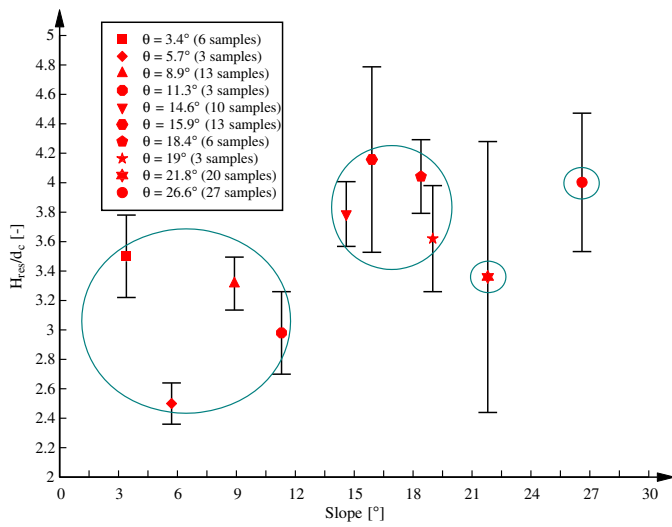


Fig. 7. Median residual energy for flat steps; four slope groups with similar behavior (black circles); error bars show standard deviation of samples

limited number of data sets. The median values should be used in conjunction with the standard deviation, enabling a sensitivity analysis of the stepped chute design. The large scatter of data might be explained by these differences but could also result from the complexity of air-water flows more generally. As pointed out, transition flows lead to larger flow instabilities, which may result in larger measurement uncertainties and larger residual energies at the channel end. Interestingly, most engineering designs are based on design discharges and not on the lower discharges, which might have instabilities resulting in larger energies to be dissipated in the stilling structure at the downstream end. These instabilities might not just be linked with increased average energy, but the energy might be incorporated in sudden energy bursts as has been found on pooled stepped spillways with $\theta = 8.9^\circ$ (Felder and Chanson 2013). Even so, the average residual energy on the pooled stepped chute for instationary discharges was comparable with the design discharge [Fig. 6(a)]; the use of a simple design guideline for such flows must underestimate the energy to be dissipated in the stilling structure. Although the present design guideline provided a simple median value and information about the data scatter, the use of physical modeling is essential to conduct systematic testing of design and nondesign flow conditions. Furthermore, it is important to

Table 3. Design Guidelines for Stepped Spillways with Embankment Slopes $3.4^\circ \leq \theta \leq 26.6^\circ$ and Flat Steps Comprising the Present Data (Table 1) and Previous Air-Water Flow Studies (Table 2)

Slope	Step characteristics	Dimensionless residual energy, H_{res}/d_c	Validity	Flow regime
3.4° – 11.3°	$0.05 \leq h \leq 0.143$ m	3.31	$0.61 \leq d_c/h \leq 4$	TRA and SK
14.6° – 19°	$0.03 \leq h \leq 0.1$ m	3.96	$1.06 \leq d_c/h \leq 4$	SK
21.8°	$0.05 \leq h \leq 0.1$ m	3.37	$0.7 \leq d_c/h \leq 2.9$	TRA and SK
26.6°	$0.03 \leq h \leq 0.1$ m	3.94	$0.69 \leq d_c/h \leq 3.6$	TRA and SK

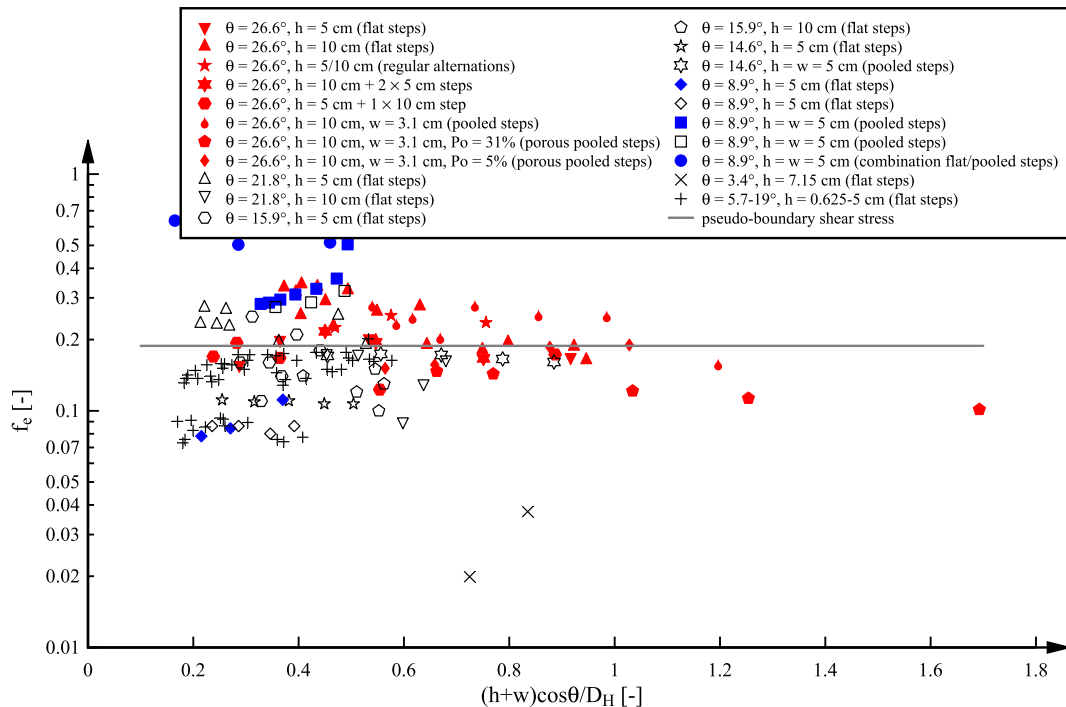


Fig. 8. Equivalent Darcy friction factors of stepped spillways with embankment dam slopes; filled symbols = data of present study, Table 1; hollow symbols = references for data are in Table 2)

identify any uncertainties. Existing data sets could be provided easily online (e.g., Felder 2013) to allow a more systematic comparison of experimental studies including air-water flow properties and further design parameters.

Flow Resistance for Flat Sloped Stepped Spillways

On stepped spillways, significant form losses take place along the steps. The flow resistance is commonly expressed in terms of the Darcy-Weisbach friction factor f_e (Chanson 2001). The friction factor characterizes a dimensionless shear stress between main stream skimming flow and cavity flow in the air-water flow region downstream of the inception point of free-surface aeration. In the present study, no uniform equilibrium flow was achieved along the stepped chutes, and the average equivalent Darcy-Weisbach friction factor was calculated in the gradually varied flow for flat, pooled, and porous pooled stepped chutes (e.g., Chanson 2001)

$$f_e = \frac{8 \times g \times S_f \times [\int_0^{Y_{90}} (1 - C) \times dy]^3}{q_w^2} \quad (9)$$

where the friction slope equals $S_f = -\partial H / \partial x$; H = total head; and x = distance in flow direction. All the data were calculated according to the air-water flow measurements. The results are summarized in Fig. 8. The friction factor is presented as a function of the dimensionless step roughness height k_s/D_H with the step cavity height k_s and the hydraulic diameter D_H or equivalent pipe diameter. Fig. 8 includes all skimming flow data for the flat sloped stepped spillways. A key finding is the close agreement of all data independent of the channel slope and discharge (Fig. 8). Apart from a few discrepancies for the spillway with the combination of flat and pooled steps and very low friction factors for the stepped chute with 3.4° , all values were in the range of $f_e = 0.1-0.4$. The data compared well with the simplified solution of a Prandtl mixing length model (Chanson et al. 2002) expressing the pseudoboundary shear stress

$$f_d = \frac{2}{\sqrt{\pi} \times K} \quad (10)$$

where f_d = equivalent Darcy friction factor estimate of the form drag; and $1/K$ = dimensionless rate of expansion of the shear layer. Eq. (10) is shown in Fig. 8 for $K = 6$.

The present findings (Fig. 8) highlighted the significant flow resistance of stepped spillways independently of channel slopes and discharges. Although a similar result was derived for gravity dam stepped chutes (Chanson et al. 2002), the present results extend the findings to typical embankment dam spillways.

Conclusion

The focus of this work was to develop a simple design criterion for residual energy for stepped chutes, with slopes typical of embankment dams, including the effects of free-surface aeration. Detailed air-water flow experiments were performed on several stepped spillway geometries with slopes between $\theta = 8.9^\circ$ and 26.6° comprising flat uniform and nonuniform configurations and flat, pooled, porous pooled steps, and a combination of flat and pooled steps. The data analyses were complemented by the reanalyses of existing air-water flow data sets, thus resulting in a comprehensive data set typical of embankment dams, $3.4^\circ \leq \theta \leq 26.6^\circ$.

For all configurations, the residual energy was estimated at the stepped chute's downstream end in the fully-developed air-water flow region. The results provided some simple design criteria in

terms of the dimensionless residual energy of stepped chutes with flat steps. For a slope of $3.4^\circ \leq \theta \leq 11.3^\circ$, the median remaining energy can be estimated at $H_{\text{res}}/d_c = 3.31$; for $14.6^\circ \leq \theta \leq 19^\circ$ as $H_{\text{res}}/d_c = 3.96$; for $\theta = 21.8^\circ$ as $H_{\text{res}}/d_c = 3.37$; and for $\theta = 26.6^\circ$ as $H_{\text{res}}/d_c = 3.94$. The guidelines are valid for a range of flow conditions comprising both transition and skimming flow regimes independently of the height of the spillway and for nonuniform gradually varied air-water flows. Overall, it is believed that a stepped design with a $1V:2.5H$ slope ($\theta = 21.8^\circ$) might be optimum in terms of residual energy to be dissipated in the downstream stilling structure. The Darcy-Weisbach friction factors were close for all stepped data ranging between $0.1 \leq f_e \leq 0.4$, with Eq. (10) providing some simple design criterion. In practice, and until further major scientific breakthrough, a sensible design approach should be favored, combining both a reasonable economical design supported by sound scientific calculations and physical observations, namely, (1) the use of the median value, (2) with a clear statement about data scatter to enable some sensitivity analyses, (3) the compulsory use of physical modeling for a wide range of design and non-design flow conditions, and (4) taking into account free-surface aeration.

Acknowledgments

The authors thank Dr. Jorge Matos (IST Lisbon) for his valuable comments. They acknowledge the technical assistance of Ahmed Ibrahim, Jason Van Der Gevel, and Stewart Matthews (The University of Queensland). The financial support of the Australian Research Council (Grants DP0878922 and DP120100481) is acknowledged.

Notation

The following symbols are used in this paper:

- C = void fraction defined as the volume of air per unit volume of air and water;
- C_{mean} = depth-averaged void fraction;
- D = empirical factor;
- D_o = dimensionless constant;
- d = equivalent clear water flow depth in air-water flows (m);
- d_c = critical flow depth (m);
- d_w = flow depth in the clear-water flow region above the inception point (m);
- F = air bubble count rate or bubble frequency (Hz);
- F_{max} = maximum air bubble count rate in a cross-section (Hz);
- F^* = Froude number expressed in terms of the step roughness;
- f_d = equivalent Darcy-Weisbach friction factor estimate of the form drag;
- f_e = equivalent Darcy-Weisbach friction factor in air-water flows;
- g = gravity constant: $g = 9.80 \text{ m/s}^2$ in Brisbane, Australia;
- H = total head (m);
- H_{max} = maximum upstream head (m) above chute toe;
- H_{res} = residual energy (m);
- h = vertical step height (m);
- K = constant inversely proportional to the rate of expansion of the mixing layer;
- K' = dimensionless integration constant;
- k_s = step cavity roughness height (m);
- L_l = longitudinal distance (m) measured from the weir crest to the inception point of free-surface aeration;
- l = horizontal step length (m);
- N = power law exponent;

P_o = porosity of pooled stepped spillway;
 q_w = water discharge per unit width (m^2/s);
 R = Reynolds number defined in terms of the hydraulic diameter;
 S_f = friction slope;
 U_w = mean flow velocity (m/s);
 V = interfacial velocity (m/s);
 V_c = critical flow velocity (m/s);
 V_{90} = characteristic interfacial velocity (m/s) in which void fraction is 90%;
 W = channel width (m);
 w = weir height in pooled stepped spillway configuration (m);
 x = distance along the channel bottom (m);
 Y_{90} = characteristic depth (m) in which void fraction is 90%;
 y = distance (m) measured normal to the invert (or channel bed);
 Δz_o = height (m) from the calculated step edge at the downstream end to the weir crest;
 δ_{BL} = boundary layer thickness (m);
 θ = angle between pseudobottom formed by the step edges and the horizontal; and
 \emptyset = probe sensor diameter (m).

References

- Amador, A., Sanchez-Juny, M., and Dolz, J. (2006). "Characterization of the nonaerated flow region in a stepped spillway by PIV." *J. Fluids Eng.*, 128(6), 1266–1273.
- Bung, D. (2011). "Developing flow in skimming flow regime on embankment stepped spillways." *J. Hydraul. Res.*, 49(5), 639–648.
- Bung, D. B. (2009). "Zur selbstbelüfteten gerinnestromung auf kaskaden mit gemäßigter neigung." Ph.D. thesis, Bergische Universität Wuppertal, Germany (in German).
- Carosi, G., and Chanson, H. (2008). "Turbulence characteristics in skimming flows on stepped spillways." *Can. J. Civil Eng.*, 35(9), 865–880.
- Chanson, H. (1994). "Hydraulics of skimming flows over stepped channels and spillways." *J. Hydraul. Res.*, 32(3), 445–460.
- Chanson, H. (2001). *The hydraulics of stepped chutes and spillways*, Balkema, Lisse, Netherlands.
- Chanson, H. (2002). "Air-water flow measurements with intrusive phase-detection probes. Can we improve their interpretation?" *J. Hydraul. Eng.*, 10.1061/(ASCE)0733-9429(2002)128:3(252), 252–255.
- Chanson, H., and Toombes, L. (2002a). "Air-water flows down stepped chutes: turbulence and flow structure observations." *Int. J. Multiphase Flow*, 28(11), 1737–1761.
- Chanson, H., and Toombes, L. (2002b). "Energy dissipation and air entrainment in a stepped storm waterway: An experimental study." *J. Irrig. Drain. Eng.*, 10.1061/(ASCE)0733-9437(2002)128:5(305), 305–315.
- Chanson, H., and Toombes, L. (2004). "Hydraulics of stepped chutes: The transition flow." *J. Hydraul. Res.*, 42(1), 43–54.
- Chanson, H., Yasuda, Y., and Ohtsu, I. (2002). "Flow resistance in skimming flows and its modelling." *Can. J. Civil Eng.*, 29(6), 809–819.
- Felder, S. (2013). "Air-water flow properties on stepped spillways for embankment dams: Aeration, energy dissipation and turbulence on uniform, non-uniform and pooled stepped chutes." Ph.D. thesis, School of Civil Engineering, Univ. of Queensland, Brisbane, Australia.
- Felder, S., and Chanson, H. (2009). "Energy dissipation, flow resistance and gas-liquid interfacial area in skimming flows on moderate-slope stepped spillways." *Environ. Fluid Mech.*, 9(4), 427–441.
- Felder, S., and Chanson, H. (2013). "Aeration, flow instabilities, and residual energy on pooled stepped spillways of embankment dams." *J. Irrig. Drain. Eng.*, 10.1061/(ASCE)IR.1943-4774.0000627, 880–887.
- Felder, S., and Chanson, H. (2014a). "Air-water flows and free-surface profiles on a non-uniform stepped chute." *J. Hydraul. Res.*, 52(2), 253–263.
- Felder, S., and Chanson, H. (2014b). "Effects of step pool porosity upon flow aeration and energy dissipation on pooled stepped spillways." *J. Hydraul. Eng.*, 10.1061/(ASCE)HY.1943-7900.0000858, 04014002.
- Frizell, K. W., Renna, F. M., and Matos, J. (2013). "Cavitation potential of flow on stepped spillways." *J. Hydraul. Eng.*, 10.1061/(ASCE)HY.1943-7900.0000715, 630–636.
- Gonzalez, C. A. (2005). "An experimental study of free-surface aeration on embankment stepped chutes." Ph.D. thesis, Dept. of Civil Engineering, Univ. of Queensland, Brisbane, Australia.
- Gonzalez, C. A., and Chanson, H. (2006). "Flow characteristics of skimming flows in stepped channels." *J. Hydraul. Eng.*, 10.1061/(ASCE)0733-9429(2006)132:5(537), 537–539.
- Gonzalez, C. A., and Chanson, H. (2007). "Hydraulic design of stepped spillways and downstream energy dissipators for embankment dams." *Dam Eng.*, 17(4), 223–244.
- Gonzalez, C. A., and Chanson, H. (2008). "Turbulence and cavity recirculation in air-water skimming flows on a stepped spillway." *J. Hydraul. Res.*, 46(1), 65–72.
- Guenther, P., Felder, S., and Chanson, H. (2013). "Flow aeration, cavity processes and energy dissipation on flat and pooled stepped spillways for embankments." *Environ. Fluid Mech.*, 13(5), 503–525.
- Hunt, S. L., and Kadavy, K. C. (2010). "Energy dissipation on flat-sloped stepped spillways: Part 1. Upstream of the inception point." *Trans. ASABE*, 53(1), 103–109.
- Hunt, S. L., Kadavy, K. C., and Hanson, G. J. (2014). "Simplified design methods for moderate-sloped stepped chutes." *J. Hydraul. Eng.*, 10.1061/(ASCE)HY.1943-7900.0000938, 04014062.
- Matos, J. (2001). "Onset of skimming flow on stepped spillways." *J. Hydraul. Eng.*, 10.1061/(ASCE)0733-9429(2001)127:6(519), 519–525.
- Meireles, I., and Matos, J. (2009). "Skimming flow in the nonaerated region of stepped spillways over embankment dams." *J. Hydraul. Eng.*, 10.1061/(ASCE)HY.1943-7900.0000047, 685–689.
- Ohtsu, I., Yasuda, Y., and Takahashi, M. (2004). "Flow characteristics of skimming flows in stepped channels." *J. Hydraul. Eng.*, 10.1061/(ASCE)0733-9429(2004)130:9(860), 860–869.
- Takahashi, M., and Ohtsu, I. (2012). "Aerated flow characteristics of skimming flow over stepped chutes." *J. Hydraul. Res.*, 50(4), 427–434.
- Takahashi, M., Yasuda, Y., and Ohtsu, I. (2008). "Flow patterns and energy dissipation over various stepped chutes." *J. Irrig. Drain. Eng.*, 10.1061/(ASCE)0733-9437(2008)134:1(114), 114–116.
- Thorwarth, J. (2008). "Hydraulics of pooled stepped spillways—Self-induced unsteady flow and energy dissipation." Ph.D. thesis, Univ. of Aachen, Germany (in German).